

## Supplementary Information

### Rhodium Growth on Cu<sub>2</sub>S Nanocrystals Yielding Hybrid Nanoscale Inorganic Cages and Their Synergetic Properties

Kathy Vinokurov<sup>1,3</sup>, Yehonadav Bekenstein<sup>2,3</sup>, Vitaly Gutkin<sup>3</sup>, Inna Popov<sup>3</sup>, Oded Millo<sup>2,3</sup> and Uri Banin<sup>1,3\*</sup>

<sup>1</sup> The Institute of Chemistry, The Hebrew University of Jerusalem, Jerusalem 91904, Israel

<sup>2</sup> Racah Institute of Physics, The Hebrew University of Jerusalem, Jerusalem 91904, Israel

<sup>3</sup> The Center for Nanoscience and Nanotechnology, The Hebrew University of Jerusalem, Jerusalem 91904, Israel

\* E-mail: uri.banin@mail.huji.ac.il

Supplementary information provides details on materials and methods, on X-ray Photoelectron Spectroscopy (XPS) and Scanning Tunneling Spectroscopy (STS) measurements; comment on XPS data fittings; XPS analysis of Rh-Cu<sub>2</sub>S and Ru-Cu<sub>2</sub>S hybrid cages; summary table of XPS data regarding RuRh-Cu<sub>2</sub>S hybrid cages.

#### Materials

The following chemicals (from Aldrich Chemical Co.) were used without further purification: Copper(II) acetylacetonate (Cu(acac)<sub>2</sub>, 99.99%), Ruthenium(III) acetylacetonate (Ru(acac)<sub>3</sub>, 97%), Rhodium(III) acetylacetonate (Rh(acac)<sub>3</sub>, 97%), dodecanthiol (≥98%), octadecylamine (ODA, 98%), diphenylether (≥99%), 1,2-dichlorobenzene (Anhydrous, 99%), neocuproine, phenanthroline (≥99%), chloroform (Anhydrous, 99%), isopropanol (Anhydrous, 99.5%). Standard Schlenk and glove box techniques for inert chemical treatments were employed throughout.

#### Methods

##### 1. X-ray Photoelectron Spectroscopy

The XPS measurements were performed with a Kratos AXIS Ultra X-ray photoelectron spectrometer (Kratos Analytical, Manchester, UK). Spectra were

acquired using the Al-K $\alpha$  monochromatic X-ray source (1,486.7 eV) with 0° take off angle (normal to analyzer). The vacuum pressure in the analyzing chamber was maintained at  $\sim 2 \cdot 10^{-9}$  Torr during the acquisition process. The survey spectra were collected with pass energy 160 eV, and 0.5 eV step size, dwell time 250 ms. High resolution XPS spectra were collected for Rh 3d, Ru 3d, Cu 2p, 2p, O 1s, C 1s and Au 4f peaks, with pass energy 20 eV and 0.1 eV step size, dwell time 1000 ms. Data analyses were done using Kratos Vision (Kratos Analytical Ltd.) processing software and CasaXPS (Casa Software Ltd.). The binding energies were calibrated using C 1s peak energy as 285.0 eV.<sup>1</sup>

## **2. Scanning Tunneling Microscopy and Spectroscopy**

For the STS study, the nanoparticles solutions were drop cast onto a flame annealed Au(111) substrate and let dry after which the samples were promptly inserted into our homemade STM. The STM measurements were performed at room temperature, using Pt-Ir tips, in high vacuum environment. Tunneling I-V characteristics were acquired after positioning the STM tip at different locations above individual nanoparticles, realizing a double barrier tunnel junction (DBTJ) configuration,<sup>2</sup> and disabling momentarily the feedback loop. In general, care was taken to retract the tip as far as possible from the nanoparticles, so that the applied tip-substrate voltage would fall mainly on the tip- nanoparticles junction rather than on the nanoparticles-substrate junction whose properties (capacitance and tunneling resistance) are determined by the layer of organic capping ligands (dodecanethiol). By this, voltage division induced broadening effects are minimized and the measured gaps correspond well to the real SC gaps.<sup>3, 4</sup> However, when studying single electron tunneling (SET) effects for the metallic cages (either empty or in the hybrids), the tip- nanoparticles distance was varied in order to verify the effect of changing the ‘residual fractional charge.’<sup>2</sup> The dI/dV-V tunneling spectra, proportional to the local tunneling density of states (DOS), were numerically derived from the measured I-V curves. The topographic images were acquired with current and sample-bias set values of  $I_s \cong 0.1 \text{ nA}$  and  $V_b \cong 1 \text{ V}$ .

### **Characterization**

#### **1. X-ray Photoelectron Spectroscopy**

XPS measurements show the characteristic binding energies (BE) of each element according to its compound and oxidation state. For the studied transition metals the following peaks were observed:

- a) The peaks of Rh  $3d_{5/2}$  were observed at 307.4 eV, which corresponds to Rh(0) species, and at 308.1 eV that corresponds to its oxidized form, such as - Rh<sub>2</sub>O<sub>3</sub>. The peak of Rh oxidized form is sometimes followed by the shoulder at 309.1 eV.
- b) The peak of Ru  $3d_{3/2}$  appears on the same energy region as C 1s peak. Hence, the ruthenium fittings include number of Ru  $3d_{3/2}$  doublets, overlapped with C 1s peaks. The peaks positions of Ru  $3d_{5/2}$  at 280.3 eV and 281.1 eV are associated with Ru(0) and RuO<sub>2</sub> species respectively. Therefore, the positions of Ru  $3d_{3/2}$  at 284.5 eV and 285.3 eV are overlapped with C 1s at 285 eV and 286.5 eV, which correspond to C-H and C-O bonds.

## 2. XPS Results

a. XPS elemental analysis of Rh-Cu<sub>2</sub>S hybrid cages exposed to air during the workup procedure.

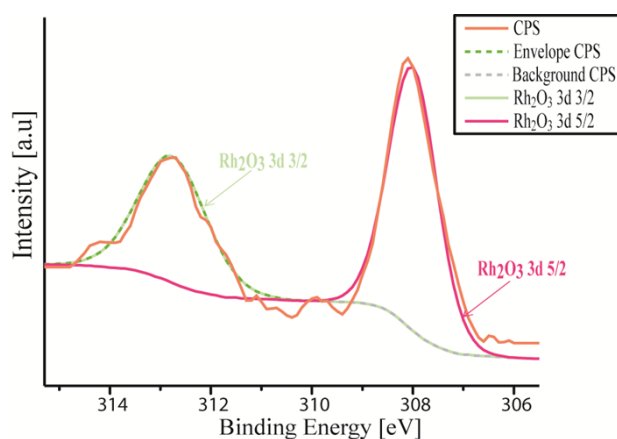


Figure S1: XPS analysis of Rh-Cu<sub>2</sub>S hybrid cages. High-resolution XPS spectra for Rh  $3d_{5/2}$  and Rh  $3d_{3/2}$  peaks fit to Rh<sub>2</sub>O<sub>3</sub> components decorating Cu<sub>2</sub>S nanocrystal edges.

b. XPS elemental analysis of Rh-Cu<sub>2</sub>S hybrid cages kept under inert atmosphere during the entire process.

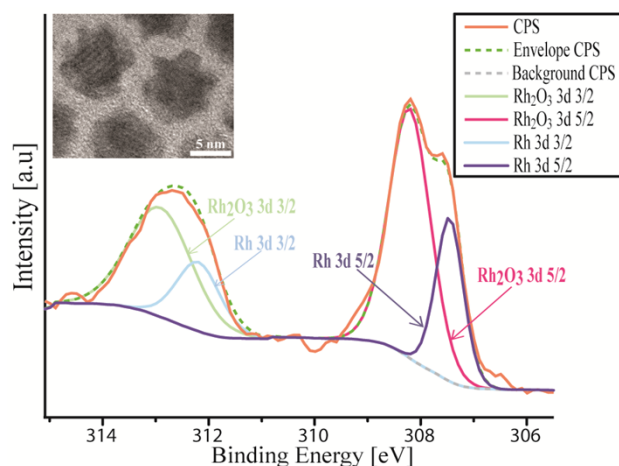


Figure S2: XPS analysis of Rh-Cu<sub>2</sub>S hybrid cages. High-resolution XPS spectra for Rh 3d<sub>5/2</sub> and Rh 3d<sub>3/2</sub> peaks and fit to Rh(0) and Rh<sub>2</sub>O<sub>3</sub> components decorating Cu<sub>2</sub>S nanocrystal edges. Inset shows TEM image of these cages.

c. XPS elemental analysis of Ru-Cu<sub>2</sub>S hybrid cages exposed to air during the workup procedure.

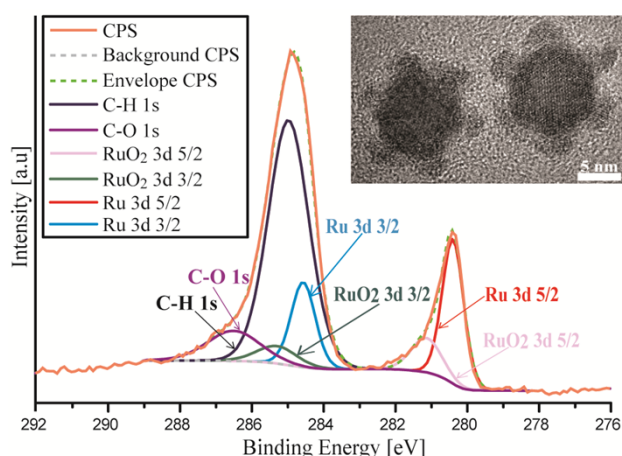


Figure S3: High resolution XPS spectrum for Ru 3d<sub>5/2</sub> and Ru 3d<sub>3/2</sub> peaks (overlapped with C 1s peaks), and fit to Ru(0) and RuO<sub>2</sub> components decorating Cu<sub>2</sub>S edges. Inset shows HRTEM images of the Ru-Cu<sub>2</sub>S cages.

d. Summary of XPS elemental analysis results of RuRh-Cu<sub>2</sub>S hybrid cages exposed to air during the workup procedure.

Element	Position [eV]	% Area	Element	Position [eV]	% Area
Ru 3d 5/2	280.4	17.5	Rh 3d 5/2	307.4	6.4
Ru 3d 3/2	284.6	11.6	Rh 3d 3/2	312.2	4.3
RuO <sub>2</sub> 3d 5/2	281.2	2.4	Rh <sub>2</sub> O <sub>3</sub> 3d 5/2	308.1	43.5
RuO <sub>2</sub> 3d 3/2	285.4	1.6	Rh <sub>2</sub> O <sub>3</sub> 3d 3/2	312.8	29.0
C-H 1s	285.1	65.1	Rh <sub>2</sub> O <sub>3</sub> 3d 5/2	309.1	12.1
C-O 1s	286.6	1.9	Rh <sub>2</sub> O <sub>3</sub> 3d 3/2	314.4	4.8
Total ratio of Ru:Rh is 1:0.7 respectively					

Table S1: Summary of XPS elemental analysis results of RuRh-Cu<sub>2</sub>S hybrid cages. The presented values were collected on bi-metal cages, which were exposed to the air during the workup procedure. The presented total ratio among ruthenium and rhodium is derived from the atomic concentration % values.

### Supporting References

1. J. F. Moudler, W. F. Stickle, P. E. Sobol and K. D. Bomben, *Perkin-Elmer, Eden Prairie, MN*, 1992, 52.
2. A. E. Hanna and M. Tinkham, *Physical Review B*, 1991, **44**, 5919-5922.
3. D. Steiner, A. Aharoni, U. Banin and O. Millo, *Nano Letters*, 2006, **6**, 2201-2205.
4. P. Liljeroth, P. A. Z. van Emmichoven, S. G. Hickey, H. Weller, B. Grandidier, G. Allan and D. Vanmaekelbergh, *Physical Review Letters*, 2005, **95**.